Vidhyayana - ISSN 2454-8596
An International Multidisciplinary Peer-Reviewed E-Journal
www.vidhyayanaejournal.org
Indexed in: Crossref, ROAD & Google Scholar

5

A Data Driven Approach for Automated Brain Tumor Segmentation & Classification

Jagriti Singh[1]

[1]Assistant Professor SDBCE, Indore

Namrata Bhatt [2]

[2]Assistant Professor VIT, Indore

Sonakshi Verma[3]

[3]Assistant Professor SDBCT, Indore

Abstract:

Machine Learning and Deep Learning are finding their applications in several domains, medical and biomedical applications being one of the most critical among them. A lot of research has gone into development of data driven models for cancer detection to serve as an id for medical practitioners. Brain cancer happens to be one of the most challenging forms of cancer to detect at an early stage as part of the tumor needs to be extracted from the brain for the biopsy analysis, which further decides the direction of treatment. As malignant and benign tumours have different treatment protocols, it is of utmost importance to detect and segment brain tumours accurately at the outset to ensure successful treatment and minimize chances of mortality. This paper presents a data driven approach for segmentation and subsequent classification of brain cancer datasets based on machine learning and deep learning approaches.

Vidhyayana - ISSN 2454-8596
An International Multidisciplinary Peer-Reviewed E-Journal
www.vidhyayanaejournal.org
Indexed in: Crossref, ROAD & Google Scholar

The machine learning model employs statistical feature extraction followed by classification using a neural network model. Image filtration is employed prior feature extraction to circumvent potential effects of noise and blurring. The deep learning models employed are the multi-instance learning (MIL) and the residual network (ResNet) models. The classification accuracy of the models is 97.5, 98% and 99% for the Neural Network, MIL and ResNet models respectively.

Keywords: Brain Cancer Detection, Image Segmentation, Neural Networks, Multi Instance Learning (MIL), Residual Network (ResNet), Classification Accuracy

I. INTRODUCTION

Cancer cases are increasing worldwide primarily due to unhealthy lifestyles, poor dietary choices, lack of physical activity, increasing pollution levels and exposure to radiation [1]. Typically, the benign tumors exhibit a clear or sharp boundary with respect to the neighboring regions and have a relatively slower spreading rate compared to the malignant tumors. The malignant tumors are much more invasive and exhibit a blurred boundary or distinction and have a much faster spreading rate [2]. The brain tumors may have different origins viz. originating from the brain (termed as primary tumors) or originating somewhere else in the body and then traversing to the brain (termed as secondary tumors) [3]. The growth rate of tumors is fundamentally governed by the oncogenes termed as procto-oncogenes [4]. These genes are governing the mitosis (cell-division) and further growth of the tumor. Typically, malignant tumors are categorized into four stages [5].

Automated tools for brain tumor detection and classificaiton are developed with the aimof providing the physician with a strong second opinion regarding the presence and type of tumor [6]. Present approaches suffer from two major challenges, one being inaccuracies in classification results for relatively small datasets, and the other being large computational complexity of existing algorithms which may make the method practically infeasible in real life situations [6].

II. METHODOLOGY

The data used in the study are MR images acquired from two datasets v.i.z. Kaggle and figshare datasets [7]-[8]. feature calculation and classification is done[9].

2.1. Image Pre-Processing

The discrete version of the wavelet transform termed as the discrete wavelet transform (DWT) is used as an iterative filer in this work for de-noising images. The wavelet transform applied on a discrete sequence $x(k)$ is given by [10]:

$$X(k) \xrightarrow[DWT]{} X_{LPF}, X_{HPF} \qquad (1)$$

Here,

DWT denotes the discrete wavelet transform operation

X_{LPF} denotes the co-efficient values obtained through low pass filtering

X_{HPF} denotes the co-efficient values obtained through high pass filtering [11].

The low pass filtering co-efficients are also termed as approximate co-efficients C_A while the high pass co-efficients are termed as detailed co-efficients C_D. The co-efficient values can be computed as [12]:

$$X_{HPF}(n) = X(k)g(2l-k) \qquad (2)$$

$$X_{LPF}(n) = X(k)h(2l-k) \qquad (3)$$

The equations (2) and (3) imply that a down-sampling or decimation of the signal has occurred by a factor of 2. i.e. every other sample of the signal has been left out, thereby decimating the signal [13].

The iterative decomposition of the set of 'n' images and retention of the approximate co-efficients is implemented using the following logic [14]:

Vidhyayana - ISSN 2454-8596
An International Multidisciplinary Peer-Reviewed E-Journal
www.vidhyayanaejournal.org
Indexed in: Crossref, ROAD & Google Scholar

$$for\ (i = 1, i \leq n, i++)$$

$$\{$$

$$Image_i \xrightarrow{DWT2} CA_{i,1}, CD_{i,1}$$

$$CA_{i,1} \xrightarrow{DWT2} CA_{i,2},, CD_{i,2} \ldots$$

$$CA_{i,k-1} \xrightarrow{DWT2} CA_{i,k},, CD_{i,k}$$

$$\}$$

Here,

i denotes the i^{th} image

The subscript index 1, 2… k denotes the level of decomposition

CAdenotes the approximate co-efficients of a particular level

CDdenotes the detailed co-efficients of a particular level

DWT2 denotes the 2-dimensional discrete wavelet transform [15].

2.2. Feature Extraction

Once the segmentation is performed, the next step is the computation of critical features based on which the decision regarding the category of the image can be taken [16]. Statistical features are computed in the proposed approach since statistical features can be computed for a wide range of images without loss of generality [17]-[18]:

1. Mean or first moment: It is the average value or first moment computed as:

$$Mean\ (\mu) = \frac{1}{N}\sum_i^N f_i X_i \qquad (12)$$

Vidhyayana - ISSN 2454-8596
An International Multidisciplinary Peer-Reviewed E-Journal
www.vidhyayanaejournal.org
Indexed in: Crossref, ROAD & Google Scholar

2. Standard Deviation: It is a measure of the difference between the instantaneous value and the mean, and is given by:

$$Standard\ Deviation\ (\sigma) = \sqrt{\frac{1}{N}\sum_i^N (X_i - \mu)^2} \quad (13)$$

3. Variance: It is the square of the standard deviation and is defined as:

$$var = \sigma^2 \quad (14)$$

4. Skewness: It denotes the amount of asymmetry of the probability distribution curve with respect to the y-axis of the curve.

$$skewness = \frac{\sum_i^N (X_i - \mu)^3}{(N-1)\sigma^3} \quad (15)$$

5. Kurtosis: The kurtosis is also termed as the fourth standard moment and is mathematically computed as:

$$Kurtosis = E[\left(\frac{X-\mu}{\sigma}\right)^4] \quad (16)$$

6. Energy: The energy is also termed as the angular secondary moment and is defined as:

$$Energy = \sum_{i,j}^N |p_{i,j}|^2 \quad (17)$$

7. Contrast: It is the degree of difference among the average and differential change in illuminance and is mathematically given by:

$$Contrast = \sqrt{\frac{1}{mn}\sum_{i,j}^{m,n}[X(i,j) - Mean(i,j)]^2} \quad (18)$$

8. Entropy: It is the average information content associated with a random variable having a probability function P, and is computed as:

$$E = -P(I_{x,y}) log_2 I_{x,y} \quad (19)$$

Vidhyayana - ISSN 2454-8596
An International Multidisciplinary Peer-Reviewed E-Journal
www.vidhyayanaejournal.org
Indexed in: Crossref, ROAD & Google Scholar

9. Homogeneity: It is a statistical measure pertaining to the similarity of distributed values of a random variable, and is mathematically defined as:

$$H = \sum_{i,j}^{m,n} \frac{P_{I,J}}{1-[i-j]^2} \qquad (20)$$

10. Correlation: It is a measure of the amount of similarity among the pixel values

$$Corr_{i,j} = \sum_{i,j}^{m,n} \frac{(i-u_x)(j-\mu_j)P_{j_{x,y}}}{\sigma_x \sigma_y} (21)$$

11. Inverse difference moment: It is defined as:

$$IDM = \sum_{i,j}^{m,n} \frac{1}{1+(i-j)^2} p_{i,j} \qquad (22)$$

12. The GLCM normalizing factor is computed as:

$$N = \frac{X_{i,j}}{\sum_{i=0}^{m-1} \sum_{j=0}^{n-1} * X_{i,j}} \quad (23)$$

Here,

X_i denotes the instantaneous value of the random variable X

$I_{x,y}$ denotes an image which is a function of spatial co-ordinates (x, y)

m, n denote the pixels along x and y axes

$mean$ denotes the average illuminance of the image

X denote the distinct values in the set

f demotes the frequency distribution of the values

N denotes the total number of levels in the normalized GLCM matrix

$p_{i,j}$ denotes the normalized GLCM matrix

P_j denotes joint probability

Vidhyayana - ISSN 2454-8596
An International Multidisciplinary Peer-Reviewed E-Journal
www.vidhyayanaejournal.org
Indexed in: Crossref, ROAD & Google Scholar

Pdenotes probability

2.3. Classification

The developed algorithms are presented next [19]-[20].

Algorithm:

The training algorithm adopted in this work is given by:

Step.1: Initialize weights (w) randomly.

Step.2: Fix the maximum number of iterations (n) and compute $\rho = \frac{k_1}{k_2}$

Step.3: Update weights using gradient descent with an aim to minimize the objective function J given by [21]:

$$J = \frac{1}{m}\sum_{i=1}^{m}(v_i - v'_i)^2 \qquad (25)$$

Step.4: Compute the Jacobian Matrix $\boldsymbol{J}$given by [22]:

$$J = \begin{bmatrix} \frac{\partial^2 e_1}{\partial w_1^2} & \cdots & \frac{\partial^2 e_1}{\partial w_m^2} \\ \vdots & \ddots & \vdots \\ \frac{\partial^2 e_n}{\partial w_1^2} & \cdots & \frac{\partial^2 e_n}{\partial w_m^2} \end{bmatrix} \qquad (26)$$

Here,

The error for iteration 'i' designated by e_i is computed as:

$$e_i = (y_i - y'_i) \qquad (27)$$

Here

$y_i$is the actual value

$y'_i$is the predicted value

Vidhyayana - ISSN 2454-8596
An International Multidisciplinary Peer-Reviewed E-Journal
www.vidhyayanaejournal.org
Indexed in: Crossref, ROAD & Google Scholar

Step.5: Iterate steps (1-4) till the cost function J stabilizes or the maximum number of iterations set in step 2 are reached, whichever occurs earlier [22].

Overlapping features values with fuzzy boundaries can not be classified accurately based on hard boundary conditions. Hence the Bayes Net is applied [23].

Let, Y_L designate the output of the Y^{th} residual block, and m_L be the mapping function of the residual block and r_B be a Bernoulli random variable, then the output of the training block can be given by [24]:

$$Y_L = f(r_B * m_L(Y_{L-1}) + m_L d(Y_{L-1})) \qquad (28)$$

Here,

d denotes a temporal delay

f denotes the ReLu (Rectified Linear) activation function defined as [25]:

$$f(x) = x; x \geq 0 \qquad (29)$$

$$f(x) = 0, x < 0 \qquad (30)$$

Two cases arise out of equation (28), one when r_B takes a value of 0 and when it takes a value of 1 [26]. In case r_B takes a values of 1, the Residual block remains active in operation. In case r_B takes a values of 0, the residual block becomes inactive and input to the output with a temporal delay of d [27].

It is customary to consider the survival probability of the residual blocks as either a linear or decaying exponential given by[28]:

$$p_s = 1 - \frac{L}{K}(1 - p_K) \qquad (31)$$

Here,

K denotes the last residual block.

p_K denotes the survival probability of the last residual block [29].

Vidhyayana - ISSN 2454-8596
An International Multidisciplinary Peer-Reviewed E-Journal
www.vidhyayanaejournal.org
Indexed in: Crossref, ROAD & Google Scholar

$L$is the total number of survival blocks.

$p_s$is the survival probability of a block 30].

Although 30% of the data has been kept for testing, 20%, 25% or 35% of the entire data could have also been utilized for testing [31]-[32]:

The classification accuracy is computed as:

$$Ac = \frac{TP+TN}{TP+TN+FP+FN} (32)$$

The sensitivity or recall is computed as:

$$Se\ or\ Re = \frac{TP}{TP+FN} \quad (33)$$

The precision is computed as:

$$Pr = \frac{TP}{TP+FP} \quad (34)$$

The specificity is computed as:

$$Sp = \frac{TN}{TN+FP} \quad (35)$$

The F-measure or F-Score is computed as:

$$F - Measure = 2.\frac{Precision*Recall}{Precision+Recall} \quad (36)$$

The F-Measure can also be computed as:

$$F - Measure = \frac{TP}{TP+\frac{1}{2}(FP+FN)} \quad (37)$$

Here,

(TP): True Positive

(TN): True Negative

Vidhyayana - ISSN 2454-8596
An International Multidisciplinary Peer-Reviewed E-Journal
www.vidhyayanaejournal.org
Indexed in: Crossref, ROAD & Google Scholar

(FP): False Positive

(FN): False Negative

III. RESULTS

The data set used has been cited in [24]-[25]. The tumor classes in the training dataset are meningioma (708 images), glioma (1426 images) and pituitary tumors (930 images). The image properties on importing to Matlab workspace are:

Table 1: Image Properties

S.No.	Attribute	Value
1.	Size	224x224x1 (Grayscale)
2.	Initial Class	Unsigned integer (uint8)
3.	Class Converted	double

The images are first loaded, subsequently the pre-processing, segmentation and feature extraction is implemented. The input images are first converted from RGB to grayscale images, de-noised using the discrete wavelet transform after which the segmentation is performed. The original and segmented images for the three categories have been depicted in figure 5-7.

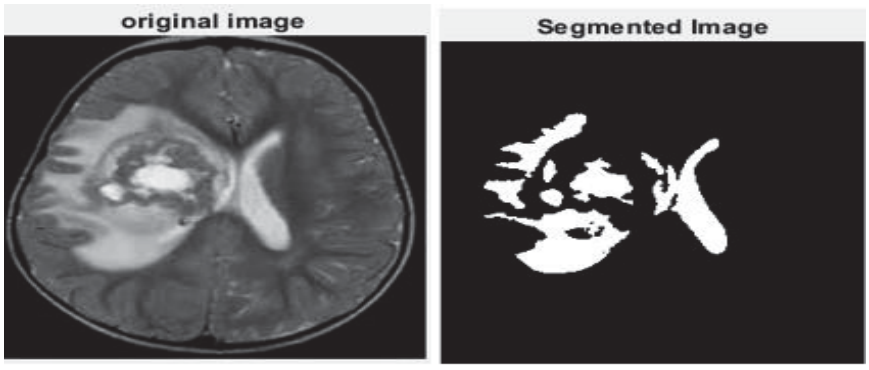

Figure 1 Original and Segmented Images for meningioma category.

Vidhyayana - ISSN 2454-8596
An International Multidisciplinary Peer-Reviewed E-Journal
www.vidhyayanaejournal.org
Indexed in: Crossref, ROAD & Google Scholar

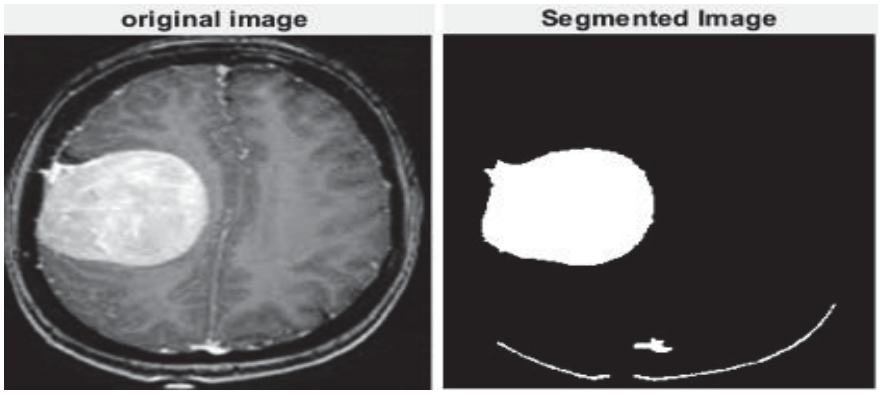

Figure 2 Original and Segmented Images for glioma Category

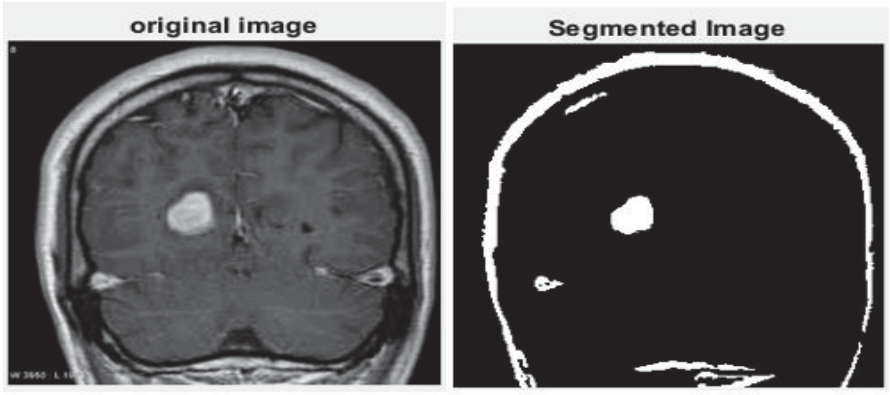

Figure 3 Original and Segmented Images for pituitary tumor Category

The segmentation of the images is followed by the computation of the features of the image. Feature extraction may be done separately for images so as to train classifiers not with the pixel information directly but rather with statistical values unique to a class of images.

Thus, the proposed approach puts forth two different approaches, one employing feature extraction and machine learning and the other using deep learning.A comparative analysis of the proposed system with respect to the existing techniques show that the proposed system outperforms the exiting techniques in terms of accuracy of classification. It can be observed from table 4 that that the proposed system attains an average accuracy 98.13% and 96.89% for the three categories of the dataset, employing the Deep Bayes Net and ResNet respectively

Vidhyayana - ISSN 2454-8596
An International Multidisciplinary Peer-Reviewed E-Journal
www.vidhyayanaejournal.org
Indexed in: Crossref, ROAD & Google Scholar

Table 2 Performance Parameters for Deep Bayes Net

Class	Accuracy%	Sensitivity Or Recall%	Specificity%	Precision%	F-Measure
meningioma	98.72	99.42	98.04	98.02	98.71%
glioma	98.38	98.30	98.46	98.44	98.36%
pituitary tumors	97.31	97.77	96.87	96.70	97.23%

Table 2 highlights the performance of the proposed system when the Deep Bayes Net has been used. It can be observed that the system attains highest accuracy in case of meningioma, followed by glioma and pituitary tumors.

Table 3 Performance Parameters for ResNet 50

Class	Accuracy%	Sensitivity Or Recall%	Specificity%	Precision%	Recall
meningioma	98.30	97.42	99.16	99.12	98.26%
glioma	98.10	98.45	97.76	97.76	98.10%
pituitary tumors	94.29	97.33	97.29	97.11	97.21%

Table 3 highlights the performance of the proposed system with ResNet 50. It can be seen that the system attains highest accuracy in case of meningioma, followed by glioma and pituitary tumors. It can also be observed that that the Deep Bayes Net performs marginally better than the ResNet 50, in terms of classification accuracy. A comparative Analysis with exiting work in the domain has been presented in table 4.

It can be observed from table 6 that both the Deep Bayes Net and the ResNet architectures outperform the benchmark techniques cited in table 6.

Table 4 Comparative Analysis w.r.t. existing work

Method	No. of Images Used	Accuracy
Phaye et al. [34]	3064	95.05
Anaraki et al. [33]	989 (Axial)	94.2
Tahir et al. [35]	3064	86
Proposed	**3064**	**98.13 (average) (Deep Bayes Net)** **96.89 (ResNet-50)**

IV. CONCLUSION

This paper presents a deep neural network-based model for brain tumor classification. The proposed scheme presents two network architectures v.i.z. the Deep Bayes Net and the ResNet-50 for multi-class classification of brain MR images. The proposed model presents a rigorous image pre-processing paradigm prior to feature computation, which makes the system more robust and immune to noise effects. The statistical feature extraction presented in this paper would be applicable to a wide range of images thereby rendering flexibility to the choice of data source and image formats. The performance metrics of the proposed system have been chosen as accuracy, sensitivity, specificity and precision. The two models attain an average accuracy of 98.13% and 96.89% along with significantly high values of the other performance

metrics. A comparative analysis has also been done with latest existing work in the domain. It has been shown that the proposed technique outperforms the existing work in terms of classification accuracy. As manual labelling the data for large datasets is extremely cumbersome and prone to errors, hence further directions of research can be exploring self supervised learning (SSL) models and techniques to reduce the complexity in labelling large datasets. The limitation of the proposed approach can be thought of as the requirement for large training datasets and tedious labelling procedures.

References

[1] World Health Organization: Cancer, Available at: https://www.who.int/health-topics/cancer#tab=tab_1, accessed July 2021.

[2] https://seer.cancer.gov/data-software/documentation/seerstat/nov2017/

[3] Sajjad M, Khan S, Muhammad K, Wu W, Ullah, Baik S. Multi-grade brain tumor classification using deep CNN with extensive data augmentation, Journal of Computational Science, Elsevier 2019, 30:174-182

[4] Comoglio PM, Trusolino L. Known and novel roles of the MET oncogene in cancer: a coherent approach to targeted therapy, Nature Reviews Cancer, 2018, 18:341–358.

[5] Wani AA, WaniMARamzan AU. Combination of needle aspiration and core needle biopsy: A new technique of stereotactic biopsy, Asian Journal of Neurosurgery, 2016, 11, 2: 94-97.

[6] Iqbal S, Khan M, Saba T, Rehman A. Computer-assisted brain tumor type discrimination using magnetic resonance imaging features, Biologic Engineering Letters, Springer 2018, 8:5–28

[7] Park C., Took M, Seong JK. Machine learning in biomedical engineering, Biomedical Engineering Letters, Springer 2018, 8:1–3.

[8] Imani M, Ghassemian H. An overview on spectral and spatial information fusion for hyperspectral image classification: Current trends and challenges, Information Fusion, Elsevier 2020, 59:59-83.

[9] Ayadi W, Elhamzi W, Charfi I, Atri M. Deep CNN for brain tumor classification, Neural Processing Letters, Springer 2021, 53: 671-700.

[10] Arunkumar N, Mohammed MA., Abd Ghani MK, Ibrahim D, Abdulhay E, Gonzalez GR, Hugo V, Albuquerque C. K-means clustering and neural network for object detecting and identifying abnormality of brain tumor, Journal of Soft Computing, Springer 2018, 23:9083–9096.

[11] KumariN. Saxena S. Review of Brain Tumor Segmentation and Classification, In: Proceedings of the 2018 International Conference on Current Trends towards Converging Technologies (ICCTCT), 2018:1-6.

[12] Ajai A. Gopalan S. Analysis of Active Contours Without Edge-Based Segmentation Technique for Brain Tumor Classification Using SVM and KNN Classifiers, In Advances in Communication Systems and Networks, Lecture Notes in Electrical Engineering, Springer 2020, 656:1-10.

[13] Song G. Huang Z, Zhao Y, Zhao X, Liu Y, Bao M, Han J, Li P. A noninvasive system for the automatic detection of gliomas based on hybrid features and PSO-KSVM, In IEEE Access, 7:13842-13855

[14] Jabber B. Rajesh K. Haritha D, Basha C, Parveen S.N. An Intelligent System for Classification of Brain Tumours with GLCM and Back Propagation Neural Network, In: Proceedings of 2020 4th International Conference on Electronics, Communication and Aerospace Technology (ICECA), 2020:21-25

[15] Deepak S Ameer PM, Brain tumor classification using deep CNN features via transfer learning, Computers in Biology and Medicine, Elsevier 2019, 111:103345.

[16] Kaldera H, Gunasekara S.R, Dissanayake M.B. Brain tumor Classification and Segmentation using Faster R-CNN, In: Proceedings of 2019 Advances in Science and Engineering Technology International Conferences (ASET), 2019:1-6.

[17] Aarthi R, Prabha K.H., Classification of brain neoplasm from multi-modality MRI with the aid of ANFIS classifier, Multidimensional Systems and Signal Processing, Springer 2021, 32:933–957

[18] Krishnammal P.M., Raja S.S., Medical image segmentation using fast discrete curvelet transform and classification methods for MRI brain images, Multimedia Tools and Applications, Springer 2020, 79:10099–10122.

[19] Deepak S, Ameer P, Automated categorization of brain tumor from mri using cnn features and svm. Journal of Ambient Intelligence and Humanized Computing, Springer 2020, 12: 8357–8369.

[20] Jayaprada S, JayaLakshmi G, Kanyakumari L, Fast Hybrid Adaboost Binary Classifier For Brain Tumor Classification, IOP Conference Series: Materials Science and Engineering, 1074: 012016.

[21] DYerukalareddy D, Pavlovskiy D, Brain Tumor Classification based on MR Images using GAN as a Pre-Trained Model, 2021 IEEE Ural-Siberian Conference on Computational Technologies in Cognitive Science, Genomics and Biomedicine (CSGB), 2021: 380-384.

[22] ShafiquMe, Naseer M, Theocharides T, Kyrkou C, Mutlu O, Orosa L, Choi J. Robust Machine Learning Systems: Challenges, Current Trends, Perspectives, and the Road Ahead, IEEE Design & Test, 37, 2, 2020:30-57

[23] Nazir M, Shakil S, Khurshid K, Role of Deep Learning in Brain Tumor Detection and Classification (2015 to 2020): A Review, Computerized Medical Imaging and Graphics, Elsevier 2021, 91: 101940,

[24] https://figshare.com/articles/dataset/brain_tumoraccessed July 2021.

[25] https://www.kaggle.com/sartajbhuvaji/brain-tumor-classification-mriaccessedJuly 2021.

[26] Manjón, J.V. MRI Pre-processing, Imaging Biomarkers, Springer 2017:63-63.

[27] Dhruv B, Mittal N, Modi M. Analysis of different filters for noise reduction in images, In proceedings of 2017 Recent Developments in Control, Automation & Power Engineering (RDCAPE), IEEE 2017:410-415.

[28] Choi H, Jeong J. Despeckling Images Using a Preprocessing Filter and Discrete Wavelet Transform-Based Noise Reduction Techniques, IEEE Sensors Journal, 2018, 18, 8:3131-3139.

[29] Zhang Y, Liu Z, Huang M, Zhu Q, Yang B. Multi-resolution depth image restoration, Machine Vision and Applications, Springer 2021, 32:65.

[30] Sarkar S, Das S, Chaudhuri S.S. Multi-level thresholding with a decomposition-based multi-objective evolutionary algorithm for segmenting natural and medical images, Applied Soft Computing, Elsevier 2017, 50:142-157.

[31] Guido R.C, A tutorial review on entropy-based handcrafted feature extraction for information fusion, Information Fusion, Elsevier 2018, 41: 161-175.

[32] Srivastava D, Rajitha B, Agarwal S, Singh S. Pattern-based image retrieval using GLCM, Neural Computing and Applications, Springer 2020, 32:10819–10832.

[33] Anaraki AK, Ayati M, Kazemi F. Magnetic resonance imaging-based brain tumor grades classification and grading via convolutional neural networks and genetic algorithms, Biocybernetics and Biomedical Engineering, Elsevier 2019, 39, 1:63-74.

[34] Phaye S, Sikka A, Dhall A, Bathula D. Dense and diverse capsule networks: Making the capsules learn better, arXiv:1805.04001, 2018:1-11.

[35] Tahir B, Iqbal S, Khan M, Saba T, Mehmood Z, Anjum A, Mahmood T. Feature enhancement framework for brain tumor segmentation and classification, Microscopy Research and Technique, Wiley Online 2019.